Available online at www.sciencedirect.com
SCIENCE DIRECT®
International Journal of Solids and Structures 42 (2005) 1923–1941
INTERNATIONAL JOURNAL OF SOLIDS and STRUCTURES
www.elsevier.com/locate/ijsolstr

Validation of an interaction law for the Eshelby inclusion problem in elasto-viscoplasticity

S. Mercier *, N. Jacques, A. Molinari

Laboratoire de Physique et Mécanique des Matériaux, I.S.G.M.P., Université de Metz, Ile du Saulcy, 57045 Metz, France

Received 29 April 2004; received in revised form 17 August 2004
Available online 23 November 2004

Abstract

The nonlinear Eshelby problem is considered for an elastic viscoplastic inclusion. An approximate solution has been proposed by [Molinari et al., 1997. On the self-consistent modelling of elastic–plastic behavior of polycrystals. Mech. Mater. 26, 43–62] who have postulated a simplified interaction law. With this interaction law, the average strain rate in the inclusion can be related to the far field loading prescribed in the matrix. In the present work, the matrix and the inclusion have elastic-viscoplastic behavior described by a nonlinear Maxwell law. Comparisons between predictions derived from the interaction law and finite element results are performed. It is observed that the approximate solution is in good agreement with numerical results as far as average strain rates and stresses are considered in the inclusion. Various inclusion shapes, material parameters and loading conditions are taken into account.

Keywords: Interaction law; Elastic-viscoplastic materials; Inclusion problem

1. Introduction

The problem of an inclusion embedded in an infinite matrix has been treated in linear elasticity by Eshelby (1957). In this work, the mechanical fields inside the inclusion are derived analytically. The key result is that the deformation inside an ellipsoidal inclusion is homogeneous. For nonlinear behaviors such as for rigid viscoplastic, elastic plastic or elastic viscoplastic materials, the deformation inside the ellipsoidal inclusion becomes heterogeneous, and no analytical solution exists. To overcome this difficulty, several authors have proposed a linearization of the material behavior through a secant, incremental or tangent way, see Hill

* Corresponding author. Tel.: +33 3 87 31 54 09; fax: +33 3 87 31 53 66.
E-mail address: mercier@lpmm.univ-metz.fr (S. Mercier).

0020-7683/$ - see front matter © 2004 Elsevier Ltd. All rights reserved.
doi:10.1016/j.ijsolstr.2004.08.016

(1965), Rice (1971), Hutchinson (1976), Molinari et al. (1987). Those models lead to the derivation of an interaction law which links the average values of mechanical fields in the inclusion to the remote homogeneous loading. Thus the average strain, stress or strain rate inside the inclusion are determined in an approximate way using the linear Eshelby solution. Those interaction laws combined with appropriate averaging schemes have been widely used to determine the macroscopic behavior of heterogeneous materials.

Few studies have been performed to validate the proposed approximate interaction laws. For viscoplastic materials, Molinari et al. (1987). have developed a tangent interaction law based on an affine linearization of the matrix behavior. Combined with a self-consistent scheme, the authors are able to predict the macroscopic behavior of polycrystalline aggregate and texture evolutions. To prove the accuracy of the proposed interaction law, Molinari et al. (2004). compared the predictions of the average strain rate inside the inclusion to values obtained by Gilormini and Germain (1987) and Gilormini and Michel (1999) with Finite Element. The matrix and the inclusion have both rigid viscoplastic behavior. The effective stress is linked to the effective strain rate through a powerlaw. A good agreement is observed for various inclusion shapes and loading conditions. As a consequence, the interaction law proposed by Molinari et al. (1987) in association with an appropriate averaging scheme can be useful to simulate the macroscopic behavior of heterogeneous material in the viscoplastic domain.

Since micromechanical viscoplastic models are efficient, the next challenge is to deal with elastic-viscoplastic heterogeneous materials. The main problem with this behavior has been illustrated by Suquet (1985). The author considers an aggregate of incompressible linear viscoelastic phases whose behaviors are represented by a Maxwell law. The macroscopic behavior of the aggregate does not follow a Maxwell law. As a consequence, the type (or the mathematical description) of the macroscopic behavior is not known a priori, which leads to a strong difficulty in micromechanics. Exact solutions, even with linear behavior, are difficult to obtain. One can mention at least two exceptions: Hashin (1969) obtained an analytical solution of the inclusion problem in linear incompressible viscoelasticity giving the homogeneous strain inside the inclusion as a function of the remote loading. Calculations are done using Laplace transform and the correspondence principle. Using also Laplace transform technique, Rougier et al. (1993) have derived an analytical solution for the macroscopic behavior of a two phase incompressible linear viscoelastic material. A self-consistent scheme is adopted for the averaging process. Since the resolution in the Laplace space is fruitful in linear viscoelasticity, some authors have tried to extend the mathematical tool to nonlinear behaviors. Masson and Zaoui (1999) have proposed a homogeneization scheme for elastic-viscoplastic materials. After linearization of the problem, they use Laplace transform technique and solve a symbolic problem in the Laplace space. The inverse transform to the time space is performed numerically with a collocation technique, see Schapery (1962). The proposed method has a high computational time-cost. Moreover, Laplace technique is only exact for nonageing linear visco-elastic behavior. In the nonlinear range where material parameters are time evolving, this induces approximations which are difficult to quantify. To avoid these drawbacks, several authors have proposed approximated interaction laws for nonlinear elastic-viscoplastic materials, Kouddane et al. (1993), Turner et al. (1994), Molinari et al. (1997), Paquin et al. (1999), Molinari (2002), Sabar et al. (2002).

The aim of the present work is to validate the interaction law proposed initially by Kouddane et al. (1993) for isotropic behavior and generalized by Molinari et al. (1997) and Molinari (2002). The material behavior is elastic-viscoplastic. The interaction law is presented in a general form. For the special case of an isotropic incompressible linear viscoelastic behavior, the results obtained with the proposed interaction law coincide with the analytical solution of the inclusion problem obtained by Hashin (1969). In the following of the paper the inclusion problem is modelled using the Finite Element software Abaqus and a detailed comparison is made with the predictions of the proposed interaction law. A power law is adopted to represent the nonlinear viscous flow of both phases and isotropic elasticity is assumed. Various inclusion shapes and loading conditions are considered. Material parameters are also varied in a large range. Results are presented for incompressible and for compressible elasticity.

2. Interaction law for elastic-viscoplastic materials

2.1. Position of the problem

Consider an inclusion embedded into an infinite matrix. Both phases have nonlinear elastic-viscoplastic behaviors. A small deformation theory is adopted. The total strain rate tensor $\underline{d}$ is split into an elastic part $\underline{d}^{\mathrm{e}}$ and a viscoplastic part $\underline{d}^{\mathrm{vp}}$.

$$\underline{d} = \underline{d}^{\mathrm{e}} + \underline{d}^{\mathrm{vp}} \tag{1}$$

The elastic part is linked to the rate of the Cauchy stress tensor $\dot{\underline{\sigma}}$ by the incremental elastic law:

$$\underline{d}^{\mathrm{e}} = (\underline{\underline{a}}^{\mathrm{e}})^{-1} : \dot{\underline{\sigma}} \tag{2}$$

where $\underline{\underline{a}}^{\mathrm{e}}$ is the fourth order tensor of elastic moduli. The viscoplastic contribution $\underline{d}^{\mathrm{vp}}$, assumed volume preserving, is related to the deviatoric Cauchy stress tensor $\underline{s}$ by

$$\underline{d}^{\mathrm{vp}} = \frac{\partial f}{\partial \underline{s}}(\underline{s}) \quad \text{or} \quad \underline{s} = \frac{\partial g}{\partial \underline{d}}(\underline{d}^{\mathrm{vp}}) \tag{3}$$

where f and g are stress or strain rate potentials respectively.

An homogeneous macroscopic strain rate $\underline{D}$ is prescribed at the remote boundary of the matrix (see Fig. 1) and induces an homogeneous Cauchy stress tensor $\underline{\Sigma}$ ($\underline{S}$ is the associated deviatoric Cauchy Stress) and an homogeneous Cauchy stress rate tensor $\dot{\underline{\Sigma}}$. Those quantities are the macroscopic mechanical fields present in the matrix far from the inclusion (the matrix is infinite). $\underline{\Sigma}$, $\dot{\underline{\Sigma}}$ and $\underline{D}$ are linked together by the elastic-viscoplastic behavior of the matrix. Let us denote $\underline{\sigma}_i$, $\dot{\underline{\sigma}}_i$ and $\underline{d}_i$ the average values of the Cauchy stress tensor, rate of Cauchy stress tensor and strain rate tensor in the inclusion; $\underline{s}_i$ and $\dot{\underline{s}}_i$ are the deviatoric stress and stress rate.

Molinari et al. (1997) and Molinari (2002) have postulated the following interaction law:

$$\underline{d}_i - \underline{D} = (\underline{\underline{A}}^{\mathrm{tg}} - (\underline{\underline{P}}^{\mathrm{tg}})^{-1})^{-1} : (\underline{s}_i - \underline{S}) + (\underline{\underline{A}}^{\mathrm{e}} - (\underline{\underline{P}}^{\mathrm{e}})^{-1})^{-1} : (\dot{\underline{\sigma}}_i - \dot{\underline{\Sigma}}) \tag{4}$$

where $\underline{\underline{A}}^{\mathrm{e}}$ stands for the fourth order tensor of the matrix elastic moduli. $\underline{\underline{A}}^{\mathrm{tg}}$ is the tensor of tangent viscoplastic moduli of the matrix, which is obtained using the viscoplastic flow law (3). Nonlinear viscoplastic behaviors are considered in the present work, therefore $\underline{\underline{A}}^{\mathrm{tg}}$ is depending on the macroscopic viscoplastic strain rate $\underline{D}^{\mathrm{vp}}$. The tensor $\underline{\underline{P}}^{\mathrm{tg}}$ (respectively $\underline{\underline{P}}^{\mathrm{e}}$) is calculated with use of Green functions related to $\underline{\underline{A}}^{\mathrm{tg}}$ (respectively $\underline{\underline{A}}^{\mathrm{e}}$). These two tensors are computed by integrating the derivative of the Green functions over the inclusion volume. For more details, one may refer to Molinari (2002).

To better understand the construction of the postulated interaction law (4), let us consider a heterogeneous medium, initially at rest, sustaining a constant overall strain rate for time $t > 0$. In the initial stage of

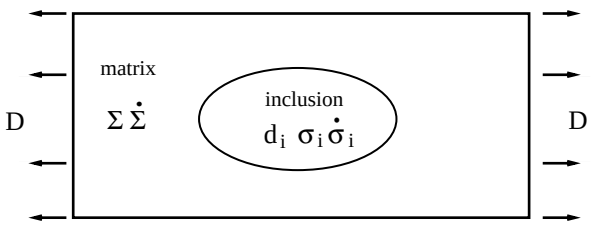

Fig. 1. Schematic representation of the inclusion problem. The matrix is infinite and the inclusion has an ellipsoidal shape. Both phases have uniform elastic-viscoplastic properties. An homogeneous strain rate tensor $\boldsymbol{D}$ is applied at the remote boundary of the matrix.

the loading, the stresses inside the phases are relatively small with important stress rates. Thus, the first term in the right hand side of Eq. (4) is small. The interaction law reduces to the one associated to a pure incremental elastic response and the classical result obtained by Eshelby (1957) in linear elasticity is retrieved. When the transient regime is over, stress rates inside the medium are vanishing. The postulated interaction law (4) reduces to the first two terms corresponding to the pure viscoplastic interaction law which has been validated by Molinari et al. (2004). The simple interaction law (4) has been postulated so as to contain the initial elastic response and also the long term viscoplastic response.

2.2. Comparison with the analytical solution proposed by Hashin (1969)

Here, we consider the case of linear viscoelasticity. The matrix and the inclusion have a local incompressible isotropic viscoelastic behavior described by the following Maxwell laws:

$$\underline{d}_i = \frac{\dot{\underline{s}}_i}{2\mu_i} + \frac{\underline{s}_i}{2\eta_i} \qquad \underline{d}_m = \frac{\dot{\underline{s}}_m}{2\mu_m} + \frac{\underline{s}_m}{2\eta_m} \tag{5}$$

where μ_i and μ_m are the elastic shear moduli, η_i and η_m are the viscous moduli for the inclusion and the matrix respectively. An homogeneous strain rate $\underline{D}$ is prescribed at the boundary of the infinite domain and corresponds to the strain rate tensor in the matrix far from the inclusion. Thus $\underline{D}$, $\underline{S}$ and $\dot{\underline{S}}$ are linked by the matrix behavior

$$\underline{D} = \frac{\dot{\underline{S}}}{2\mu_m} + \frac{\underline{S}}{2\eta_m} \tag{6}$$

Using Eqs. (5) and (6), the interaction law (4) reduces to:

$$\underline{d}_i - \underline{D} = -\frac{\underline{s}_i - \underline{S}}{3\eta_m} - \frac{\dot{\underline{s}}_i - \dot{\underline{S}}}{3\mu_m} \tag{7}$$

Kouddane et al. (1993) have mentioned that Eq. (7) coincides with the analytical solution obtained by Hashin (1969) (see Appendix A). This means that the interaction law (4) is exact for this simple case.

Eq. (7) can be written in a different form so as to introduce the viscoplastic strain rates $\underline{d}_i^{\mathrm{vp}}$ and $\underline{D}^{\mathrm{vp}}$:

$$\underline{d}_i^{\mathrm{vp}} = \frac{\underline{s}_i}{2\eta_i} \quad \underline{D}^{\mathrm{vp}} = \frac{\underline{S}_m}{2\eta_m} \tag{8}$$

This gives:

$$\dot{\underline{s}}_i = \frac{5\mu_i}{2\mu_i + 3\mu_m}\left\{\dot{\underline{S}} - 2\mu_m\left(\frac{2\eta_i + 3\eta_m}{5\eta_m}\underline{d}_i^{\mathrm{vp}} - \underline{D}^{\mathrm{vp}}\right)\right\} \tag{9}$$

With this new formulation, it is clear that the initial elastic and the long term viscoplastic strain rates are exactly evaluated. Indeed, in the initial elastic stage, $\underline{d}_i^{\mathrm{vp}}$ and $\underline{D}^{\mathrm{vp}}$ vanish and (9) provides the usual localization law for incompressible elasticity. For the long range viscoplastic stage where the stress rates vanish, (9) provides the localization law for the viscoplastic strain rates. Note that the interaction law proposed by Paquin et al. (1999) gives the same results and therefore is exact in this simple case. For comparison purpose, the interaction law proposed by Weng (1982):

$$\dot{\underline{s}}_i = \frac{5\mu_i}{2\mu_i + 3\mu_m}\left\{\dot{\underline{S}} - 2\mu_m(1-\beta)\left(\underline{d}_i^{\mathrm{vp}} - \underline{D}^{\mathrm{vp}}\right)\right\} \tag{10}$$

and the one proposed by Sabar et al. (2002):

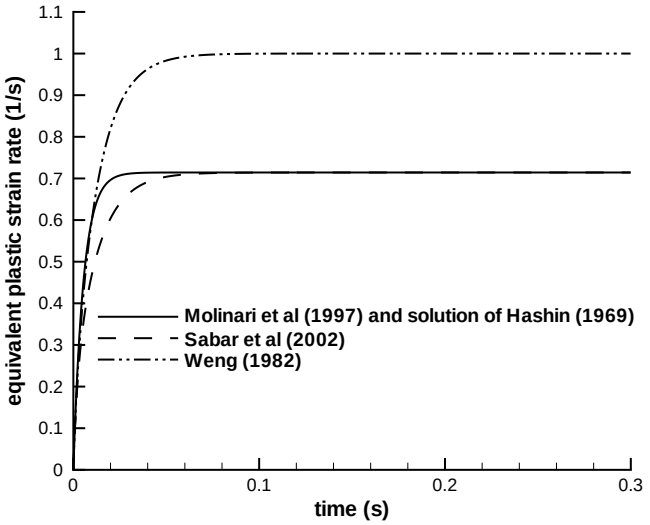

Fig. 2. Time evolution of the equivalent plastic strain rate inside the spherical inclusion. The remote loading corresponds to uniaxial tension $D_{11} = 1\,\mathrm{s}^{-1}$. The two phases have incompressible isotropic viscoelastic behavior described by a Maxwell law. The following parameters are used: $\mu_i = \mu_m = 66.66\,\mathrm{MPa}$ and $\eta_i = 0.66\,\mathrm{MPa\,s}^{-1}$, $\eta_m = 0.33\,\mathrm{MPa\,s}^{-1}$. The interaction law proposed by Molinari et al. (1997) coincides with the analytical solution obtained by Hashin (1969). Models proposed by Weng (1982) and Sabar et al. (2002) do not represent exactly this simple configuration.

$$\dot{\underline{s}}_i = \frac{5\mu_i}{2\mu_i + 3\mu_m}\left\{\dot{\underline{S}} - 2\mu_m(1-\beta)\left(\underline{d}_i^{\mathrm{vp}} - \frac{5\eta_m}{2\eta_i + 3\eta_m}\underline{D}^{\mathrm{vp}}\right)\right\} \tag{11}$$

are presented. For incompressible elastic behavior, $\beta = \frac{2}{5}$. One can observe that these relationships do not coincide with the exact result (9). The difference is illustrated on Fig. 2, which shows the time evolution of the equivalent plastic strain rate in the inclusion for the three interaction laws. The applied strain rate $\underline{D}$ at the remote boundary corresponds to uniaxial traction.

$$\underline{D} = D_0\begin{bmatrix} 1 & 0 & 0 \\ 0 & -0.5 & 0 \\ 0 & 0 & -0.5 \end{bmatrix} \tag{12}$$

The material parameters are: $\mu_i = \mu_m = 66.66\,\mathrm{MPa}$, $\eta_i = 0.66\,\mathrm{MPa\,s}^{-1}$ and $\eta_m = 0.33\,\mathrm{MPa\,s}^{-1}$. $D_0 = 1\,\mathrm{s}^{-1}$. The predictions of the three interaction laws are compared to the analytical solution, Hashin (1969). As already mentioned, the results provided by Eq. (9) coincides with the exact solution. The model proposed by Sabar et al. (2002) does not capture exactly the evolution of the strain rate for intermediate times when the viscoelastic coupling occurs. As already noticed in the literature, the model proposed by Weng (1982) is too stiff since interactions are mostly driven by elasticity.

3. Numerical modelling

When the behavior is nonlinear, there is no analytical solution of the inclusion problem. Therefore, finite element calculations have to be performed for comparison purpose. In the present work, the software ABAQUS is used. Geometric nonlinearity are disregarded since a small deformation formalism has been adopted.

Three different loading conditions have been tested. First, the strain rate loading corresponds to uniaxial tension, Eq. (12). Axisymmetric conditions are prescribed since only axisymmetric inclusions are considered in the present work (see Fig. 3). The axes of the inclusion and the loading directions are aligned. To approach the infinite extent of the matrix, a large dimension is adopted for the matrix, corresponding to thirty five times the inclusion size. The volume fraction of a spherical inclusion is $\frac{1}{42857}$. Note that a smaller domain corresponding to ten times the inclusion size is sufficient to get accurate results in axisymmetric loading. In that case, the volume fraction would have been $\frac{1}{1000}$. The material behavior is nonlinear, therefore deformation heterogeneity occurs inside the inclusion and increases when the nonlinear material response is more pronounced. Material parameters of the two phases (matrix and inclusion) can be strongly different. Important gradients can be observed near the matrix-inclusion interface. For these two reasons, the matrix and the inclusion are meshed in two parts. For the matrix, the mesh is very dense near the interface and is coarse far from the inclusion since the effect of the inclusion is vanishing, see Fig. 4. The mesh has a high density in the inclusion to capture the deformation heterogeneity. Note the refinement near the interface to deal with strong strain gradient, see Fig. 4. Table 1 summarizes the number of elements adopted for the four part mesh in the case of spherical inclusions. Different inclusion shapes are considered: spherical, oblate (aspect ratio $\lambda = 2$) and prolate (aspect ratio $\lambda = 0.5$). The corresponding meshes are presented only for spherical inclusions.

Several types of elements available in ABAQUS library have been tested: 4-node bilinear and 8-node quadratic elements with full or reduced integration. In all cases, results are identical. Therefore, 4-node bilinear elements with reduced integration (named CAX4R) are adopted. When incompressible elasticity is considered, elements with hybrid formulation (CAX4RH) are used.

A second configuration is proposed to validate the interaction law. The problem of a cylindrical inclusion of axis $\underline{3}$ embedded in an infinite matrix is simulated in plane strain conditions, see Fig. 3. The remote loading is:

$$\underline{D} = \begin{bmatrix} 1 & 0 & 0 \\ 0 & -1 & 0 \\ 0 & 0 & 0 \end{bmatrix} (s^{-1}). \tag{13}$$

Only a circular cross-section has been tested. To approach the infinite extent of the matrix, the inclusion is embedded into a cylinder of radius thirty five times the inclusion radius. The volume fraction of inclusion is

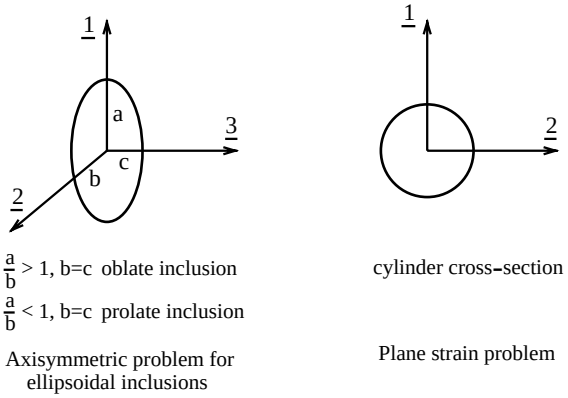

Fig. 3. Axes of the ellipsoidal inclusion are aligned with loading directions. The inclusion is axisymmetric. The remote strain rate tensor Eq. (12) corresponds to uniaxial tension. In plane strain condition, a circular cylinder is embedded into an infinite matrix. The remote strain rate is $D_{11} = 1\,s^{-1}$, $D_{22} = -1\,s^{-1}$.

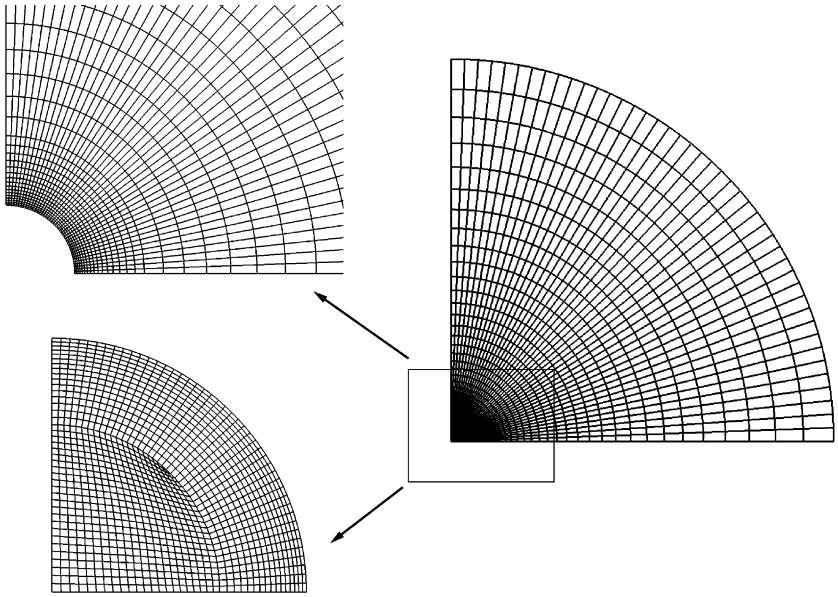

Fig. 4. View of the mesh in the inclusion and in the matrix. The mesh is dense inside the inclusion and near the interface. A coarse mesh is adopted in the matrix far from the inclusion.

Table 1
Number of elements in the inclusion and in the matrix for a spherical inclusion. The same number of elements is adopted for different loading conditions (axisymmetric traction or plane strain loading)

Spherical inclusion	Number of elements in the inclusion	Number of elements in the matrix	Number of elements in the whole domain
Total	1231	2024	3255
Near the interface	704	704	

$(\frac{1}{1225})$. Larger domain size increases the calculation time but does not improve the accuracy of the results. From the calculations, one can observe that results are accurate as soon as the volume fraction of inclusion is below $\frac{1}{1000}$. The mesh of Fig. 4 is adopted (see Table 1). For the prescribed loading, 4-node bilinear plane strain elements with reduced integration (named CPE4R) are used.

Finally, complex loadings are tested in plane strain conditions. The path corresponds to plane strain traction as in (13) followed by shear. The corresponding remote shear strain rate tensor is:

$$\underline{D} = \begin{bmatrix} 0 & 1 & 0 \\ 1 & 0 & 0 \\ 0 & 0 & 0 \end{bmatrix} (s^{-1}). \tag{14}$$

Since shear deformation does not preserve the symmetry with respect to axes $\underline{1}$ and $\underline{2}$, the whole domain has been meshed. The mesh is similar to Fig. 4, covering the whole cross-section and not only one fourth of the domain. For the proposed complex loading, in order to avoid hourglassing, fully integrated elements (named CPE4H) are used.

4. Results

In the present work, the inclusion and the matrix behaviors are described by relationships (1)–(3). The viscoplastic response (3) obeys to the J_2 flow law:

$$\sigma^{\mathrm{eq}} = \sigma_p (d^{\mathrm{eq}})^{m_p}, \quad s_{ij} = 2\eta_p(d^{\mathrm{eq}}) d_{ij}^{\mathrm{vp}} \qquad \text{with } \eta_p(d^{\mathrm{eq}}) = \frac{\sigma_p}{3}(d^{\mathrm{eq}})^{m_p - 1} \tag{15}$$

$\eta_p(d^{\mathrm{eq}})$ stands for the nonlinear viscosity of the material, $d^{\mathrm{eq}} = \sqrt{\frac{2}{3}\underline{d}^{\mathrm{vp}} : \underline{d}^{\mathrm{vp}}}$ is the equivalent plastic strain rate and $\sigma^{\mathrm{eq}} = \sqrt{\frac{3}{2}\underline{s} : \underline{s}}$ is the equivalent Cauchy stress. The scalars m_p and σ_p characterize the strain rate sensitivity and the strength of the phase (p). The elastic contribution (2) is assumed isotropic, E_p and ν_p are the Young's modulus and the Poisson's ratio respectively. The material behavior is described by a set of four parameters (m_p, σ_p, E_p and ν_p). For incompressible elasticity, the elastic behavior is characterized by the sole shear modulus $\mu_p = \frac{E_p}{3}$. The behavior of both phases is described by Eq. (5), where η_i and η_m are rate dependent and given by (15) with $p = i$ for the inclusion and $p = m$ for the matrix.

ABAQUS accounts for elastic-viscoplastic behavior of the form:

$$\sigma^{\mathrm{eq}} = \sigma_p (d^{\mathrm{eq}} + d_{\mathrm{op}})^{m_p} \tag{16}$$

where d_{op} is a strain rate threshold which we shall take as very small ($d_{\mathrm{op}} = 10^{-20}\,\mathrm{s}^{-1}$ for $m_p = 0.2$). Although the viscoplastic flow is described here by the nonNewtonian law (15), it is worth noting that the interaction law (4) applies for a general viscoplastic flow law of the form (3).

4.1. Axisymmetric traction

The aspect ratio of the inclusion is defined by $\lambda = \frac{a}{b}$ (see Fig. 3). The components of the macroscopic strain rate at the remote boundary is given by (12) with $D_0 = 1\,\mathrm{s}^{-1}$. From Eqs. (1)–(3) and (15), the time evolution of the average value of the strain rate inside the inclusion can be determined by using the interaction law (4). Finite element calculations performed on the same configuration provide the local strain rate inside the inclusion, which is nonuniform for nonlinear behaviors. Thus, a comparison between mechanical fields calculated by the interaction law (4) and the average, maximum and minimum fields obtained by FE is proposed. The average value of the equivalent plastic strain rate is defined as

$$\langle d_{\mathrm{FE}}^{\mathrm{eq}} \rangle = \frac{1}{\Omega} \int_{\Omega} d^{\mathrm{eq}}\, \mathrm{d}\Omega \tag{17}$$

where Ω is the volume of the inclusion. The subscript "FE" refers to Finite Element results.

4.1.1. Incompressible elasticity

4.1.1.1. Spherical inclusion. As stated in Appendix A, results obtained via the interaction law coincide with the analytical solution when the linear behavior $m_i = m_m = 1$ is considered, so does also the FE calculations. Results are not presented here.

In the following calculations, we have arbitrary chosen: $\sigma_m = 1\,\mathrm{IS}$ (International System Units) and $E_i = E_m = 200\,\mathrm{MPa}$ (thus for incompressible elasticity, $\mu_i = \mu_m = 66.66\,\mathrm{MPa}$). In Fig. 5, a low strain rate sensitivity $m_i = m_m = m = 0.05$ and a strong strength difference $\sigma_i = 0.1\sigma_m$ are considered. It is observed that the average viscoplastic and total strain rates inside the inclusion based on the relationship (4) are getting close to the FE results. Note that a closer agreement would be obtained for a larger strain rate sensitivity m, all other parameters being fixed. By comparing Fig. 5(a) and (b), it is observed that the long term response is purely viscoplastic. Results obtained by Molinari et al. (2004) using the rigid viscoplastic interaction law (no elasticity) are retrieved. Since Molinari et al. (2004) have concluded that for rigid viscoplastic

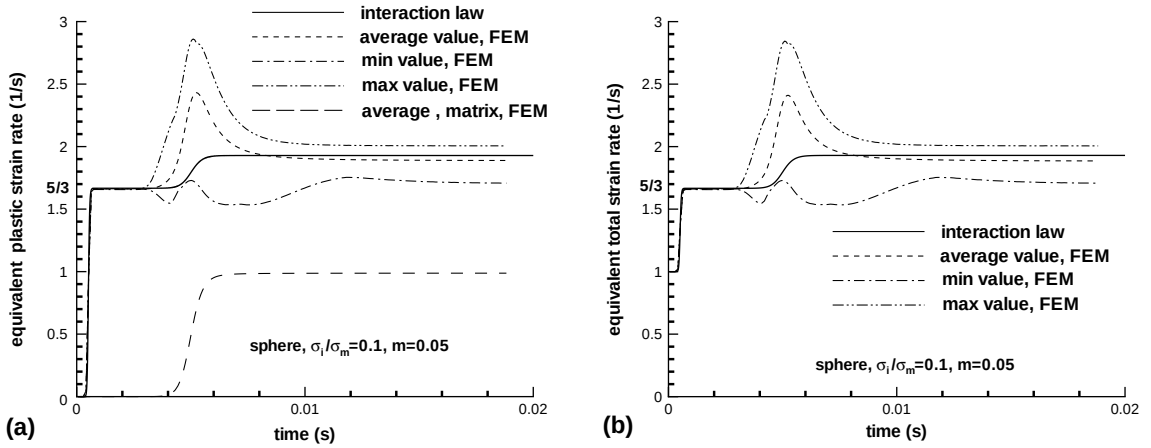

Fig. 5. Time evolution of the equivalent plastic and total strain rate in a soft spherical inclusion. Predictions based on the interaction law (4) are compared with FE simulations. The loading is axisymmetric and corresponds to uniaxial traction. Inclusion and matrix are incompressible with same elastic behavior. The following material and loading parameters are used: $m = 0.05$, $\mu = 66.66\,\text{MPa}$, $\sigma_m = 1$ IS, $\sigma_i = 0.1\sigma_m$, $D_0 = 1\,\text{s}^{-1}$.

materials the interaction law is able to capture the mean strain rate inside the inclusion, it is clear that predictions based on relationship (4) will be close to FE results for large times when elastic strain rates vanish. The matrix being harder than the inclusion, the matrix remains elastic at the beginning of the loading. The inclusion is initially strained in the elastic domain but rapidly the elastic response is replaced by the elastic-viscoplastic one, see Fig. 5(a) and (b). This stage of the deformation process is represented by the first plateau in Fig. 5 with level of the equivalent plastic and total strain rates equal to $\frac{5}{3}$. This level represents the classical equivalent strain rate in a void when the matrix remains elastic, the equivalent strain rate at the remote boundary of the matrix being unity. In the present example, the inclusion is much softer than the matrix and behaves as a void. On the plateau, the inclusion deforms in the viscoplastic domain and the equivalent plastic and total strain rates must reach the specific value $\frac{5}{3}$. This interesting case is perfectly predicted by the interaction law (4) and coincides with FE results. Except for the transient stage corresponding to the matrix transition from elastic to viscoplastic, the average value of the plastic and total strain rates inside the inclusion are accurately predicted.

When the inclusion is harder than the matrix ($\sigma_i = 10\sigma_m$) and for $m = 0.5$, Fig. 6 shows that the average plastic strain rate in the inclusion calculated with the interaction law (4) is in reasonable agreement with the average value obtained by FE. The prediction based on the interaction law (4) is close to the maximum value of the equivalent strain rate calculated by ABAQUS. A maximum error of five percent occurs during the long range viscoplastic response. This result has already been obtained by Molinari et al. (2004). To reduce the discrepancy, Molinari and Toth (1994) have proposed to introduce in the interaction law a tuning parameter calibrated with use of FE calculations.

In Fig. 7, strain rate sensitivities for the two phases are different $m_i = 0.05$ and $m_m = 0.2$. The inclusion is softer than the matrix $\sigma_i = 0.5\sigma_m$. The average value of the equivalent plastic strain rate given by the interaction law (4) is very similar to the average value calculated with ABAQUS.

All the previous calculations were performed with the same elastic behavior. Fig. 8 shows comparisons when the elastic moduli of the phases are different. The spherical inclusion is harder than the matrix $\sigma_i = 1.5\sigma_m$. Identical strain rate sensitivities are considered $m = 0.2$. In Fig. 8(a), the elastic modulus of the inclusion is ten times larger than the elastic modulus of the matrix, $\mu_i = 10\mu_m$ with $\mu_m = 66.66\,\text{MPa}$. In Fig. 8(b), the elastic moduli of the phases are: $\mu_i = 0.1\mu_m$, $\mu_m = 66.66\,\text{MPa}$. It is observed that the

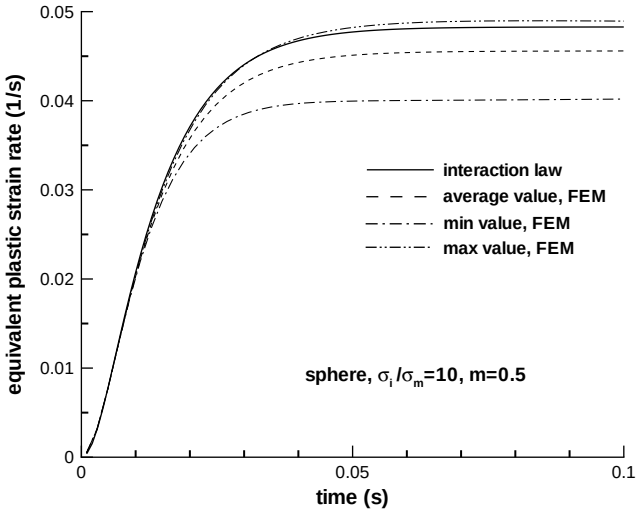

Fig. 6. Time evolution of the equivalent plastic strain rate in a hard spherical inclusion. The loading is axisymmetric and corresponds to uniaxial traction. Inclusion and matrix are incompressible with same elastic behavior. The following material and loading parameters are used: $m = 0.5$, $\mu = 66.66\,\mathrm{MPa}$, $\sigma_m = 1\,\mathrm{IS}$, $\sigma_i = 10\sigma_m$, $D_0 = 1\,\mathrm{s}^{-1}$.

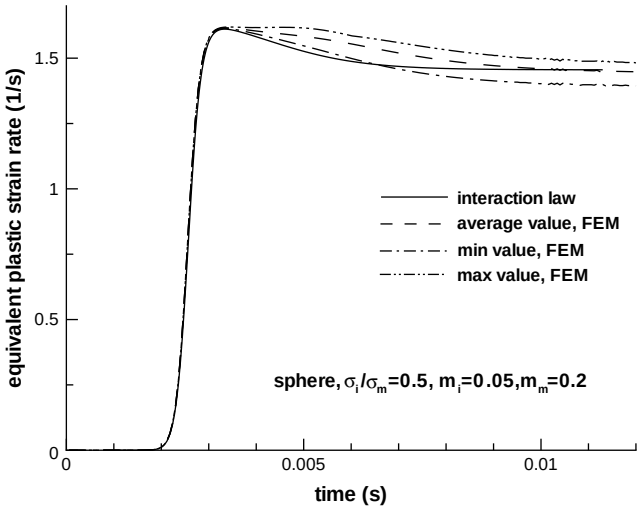

Fig. 7. Evolution of the equivalent plastic strain rate in a soft spherical inclusion. The loading is axisymmetric and corresponds to uniaxial traction. Both phases have the same incompressible elastic behavior. The phases have different strain rate sensitivities. The following material and loading parameters are used: $m_i = 0.05$, $m_m = 0.2$, $\mu = 66.66\,\mathrm{MPa}$, $\sigma_m = 1\,\mathrm{IS}$, $\sigma_i = 0.5\sigma_m$, $D_0 = 1\,\mathrm{s}^{-1}$.

predictions obtained with the interaction law (4) are in agreement with the average value obtained by FE simulations, even at intermediate times where elastic behavior plays a crucial role. The response for large times is identical in Fig. 8(a) and (b) since the long term response is viscoplastic (vanishing elastic strain rate). As a consequence, we can argue that the interaction law (4) provides reasonable predictions for heterogeneous elastic properties.

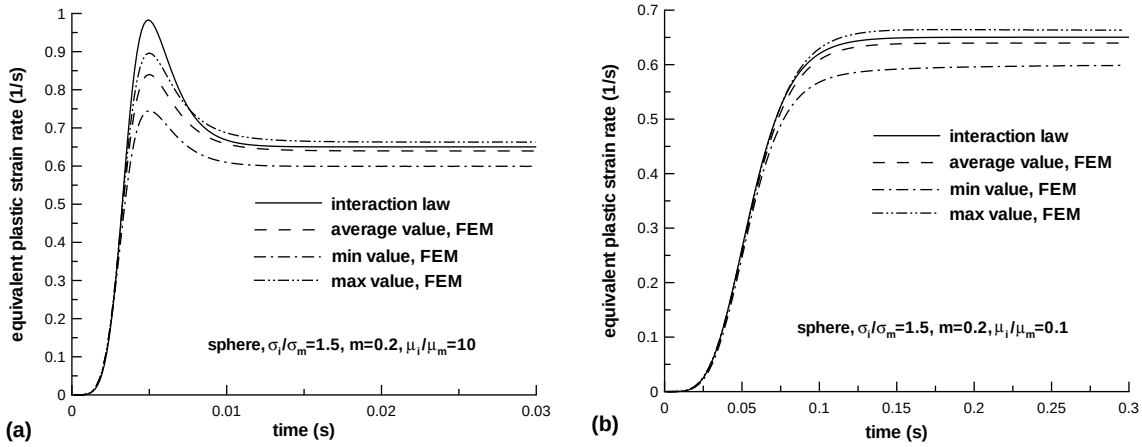

Fig. 8. Evolution of the equivalent plastic strain rate in a hard spherical inclusion. The loading is axisymmetric and corresponds to uniaxial traction. The incompressible elasticity is different for the two phases. The following material and loading parameters are used. Two cases are considered: (a) $\mu_i = 666.6\,\text{MPa}$, $\mu_m = 66.66\,\text{MPa}$, (b) $\mu_i = 6.666\,\text{MPa}$, $\mu_m = 66.66\,\text{MPa}$. Other parameters are: $m = 0.2$, $\sigma_m = 1\,\text{IS}$, $\sigma_i = 1.5\sigma_m$, $D_0 = 1\,\text{s}^{-1}$.

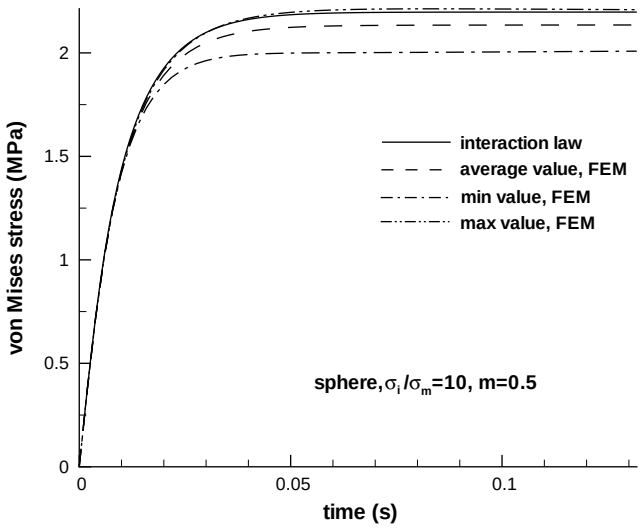

Fig. 9. Evolution of the von Mises stress in a hard spherical inclusion. Configuration and material parameters are those of Fig. 6. Note that stress differences are lower compared to strain rate differences.

Fig. 9. presents the time evolution of the flow stress σ^{eq} in the inclusion for the configuration of Fig. 6. Differences between stress predictions derived from the interaction law and FE calculations are less pronounced than plastic strain rate differences, see Fig. 6. This is due to the fact that the strain rate sensitivity has lower value than unity in the flow law.

To summarize, for soft inclusion, differences occurs mainly at intermediate times when the matrix starts to plastify. For hard inclusion, differences are observed mostly for large times, when viscoplastic strain rate is dominant with respect to elastic strain rate.

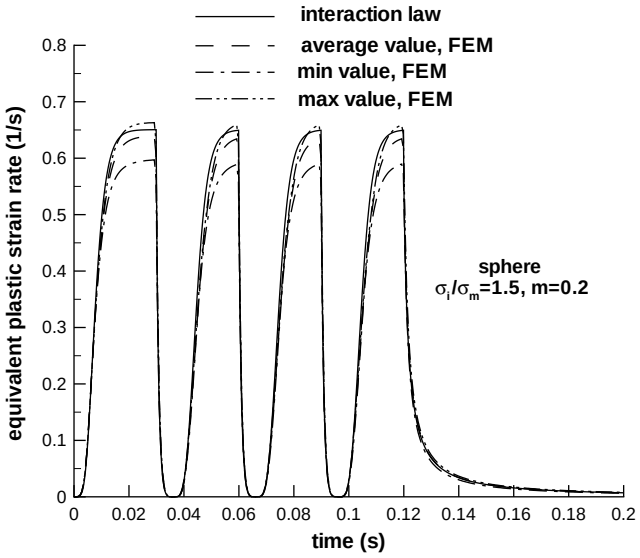

Fig. 10. Time evolution of the equivalent plastic strain rate in a hard spherical inclusion. Uniaxial traction-compression is prescribed at the remote boundary. Inclusion and matrix are incompressible with the same elastic behavior. The following material and loading parameters are used: $m = 0.2$, $\mu = 66.66\,\text{MPa}$, $\sigma_m = 1\,\text{IS}$, $\sigma_i = 1.5\sigma_m$.

4.1.1.2. Cyclic loading. The inclusion is harder than the matrix ($\sigma_i = 1.5\sigma_m$) with same strain rate sensitivity $m = 0.2$. Both phases have the same incompressible elastic behavior defined by $\mu = 66.66\,\text{MPa}$. Cyclic loading is prescribed at the remote boundary. The cycle is defined as follows: for time up to $t = 0.03\,\text{s}$, the far field strain rate tensor is defined by (12) with $D_0 = 1\,\text{s}^{-1}$. For time in the range $[0.03\,\text{s}, 0.06\,\text{s}]$, the reverse loading corresponding to axisymmetric compression with $D_0 = -1\,\text{s}^{-1}$ is considered. In Fig. 10, the time evolution of the equivalent plastic strain rate is presented for two cycles. As for monotonic loading, good results are obtained for cyclic loading with the interaction law (4). Note that for time larger than $t = 0.12\,\text{s}$, the loading has been relaxed by taking the far field strain rate equal to zero.

4.1.1.3. Prolate and oblate inclusions. To validate the interaction law (4), comparisons were also performed for oblate and prolate inclusions. An oblate ellipsoidal inclusion (aspect ratio $\lambda = 2$) is first considered. In Fig. 11, the inclusion is softer than the matrix ($\sigma_i = 0.5\sigma_m$). The strain rate sensitivity of the two phases is $m = 0.05$. As for spherical inclusions, the predictions of the interaction law and those of FE calculations coincide at the beginning of the loading and are in close agreement for large times when the deformation of both phases is purely viscoplastic (negligible elastic strain rate). At intermediate times, a difference exists. Next, an hard prolate ellipsoidal inclusion (aspect ratio $\lambda = 0.5$, $\sigma_i = 1.5\sigma_m$) is considered. The strain rate sensitivity is identical for both phases and equal to $m = 0.2$. The results obtained with the two approaches (interaction law and FE) are quite similar, see Fig. 12. As for spherical inclusions and from other simulations not presented here, one can observe that the difference between predictions of the interaction law (4) and the average values obtained by FE calculations, increases with large strength ratio and with small strain rate sensitivity.

4.1.2. Compressible elasticity

In Fig. 13, the two phases have the same elastic behavior defined by $E = 200\,\text{MPa}$, $\nu = 0.3$. Other parameters are identical to those of Fig. 7. It is observed that the quality of predictions is preserved when compressible elasticity is considered. Others results for compressible elasticity are not presented since conclusions and observations drawn for incompressible elasticity are still valid.

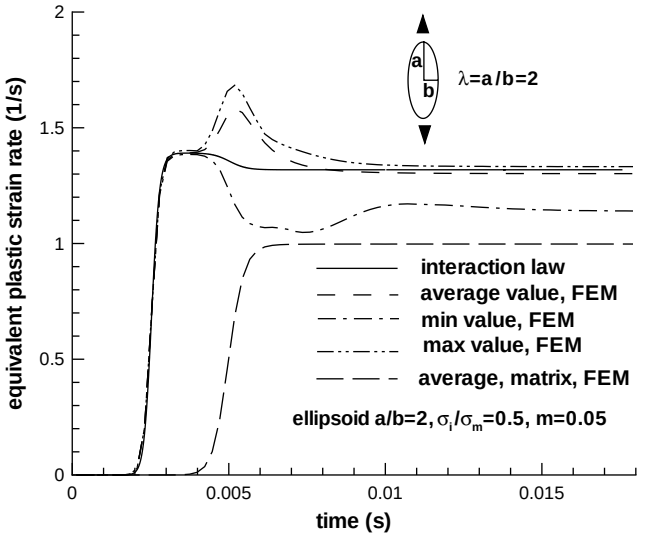

Fig. 11. Evolution of the equivalent plastic strain rate in a soft oblate ellipsoidal inclusion. The aspect ratio is $\lambda = 2$. The loading is axisymmetric and corresponds to uniaxial traction. Both phases have the same incompressible elastic behavior. The following material and loading parameters are used: $m = 0.05$, $\mu = 66.66\,\mathrm{MPa}$, $\sigma_m = 1\,\mathrm{IS}$, $\sigma_i = 0.5\sigma_m$, $D_0 = 1\,\mathrm{s}^{-1}$.

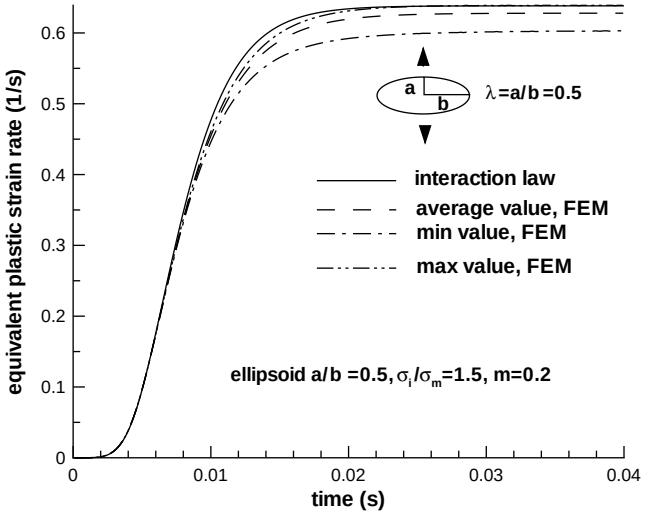

Fig. 12. Evolution of the equivalent plastic strain rate in a hard prolate ellipsoidal inclusion. The aspect ratio is $\lambda = 0.5$. The loading is axisymmetric and corresponds to uniaxial traction. Both phases have the same incompressible elastic behavior. The following material and loading parameters are used: $m = 0.2$, $\mu = 66.66\,\mathrm{MPa}$, $\sigma_m = 1\,\mathrm{IS}$, $\sigma_i = 1.5\sigma_m$, $D_0 = 1\,\mathrm{s}^{-1}$.

4.2. Plane strain

4.2.1. Monotonic loading

A second configuration is presented to validate the interaction law (4). A cylindrical inclusion of axis $\underline{3}$ is embedded into an infinite matrix (see Fig. 3) and deformed in plane strain conditions. The strain rate tensor

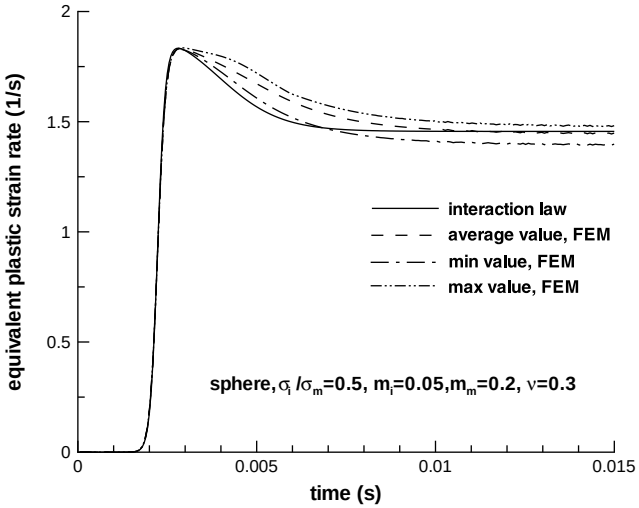

Fig. 13. Evolution of the equivalent plastic strain rate in a soft spherical inclusion. The loading is axisymmetric and corresponds to uniaxial traction. Both phases have the same compressible elastic behavior. The following material and loading parameters are used: $m_i = 0.05$, $m_m = 02$, $E = 200\,\text{MPa}$, $v = 0.3$, $\sigma_m = 1\,\text{IS}$, $\sigma_i = 0.5\sigma_m$, $D_0 = 1\ \text{s}^{-1}$.

applied at the remote boundary is given by (13). To approach the cylindrical inclusion, an oblate ellipsoidal inclusion with a large aspect ratio $c/a = 100, a = b$ is considered, see Fig. 3. The average value of the equivalent plastic strain rate inside the inclusion is defined as

$$\langle d^{\text{eq}}_{\text{FE}} \rangle = \frac{1}{S} \int_S d^{\text{eq}}\, \text{d}S \tag{18}$$

where S is the cross-section of the circular cylinder.

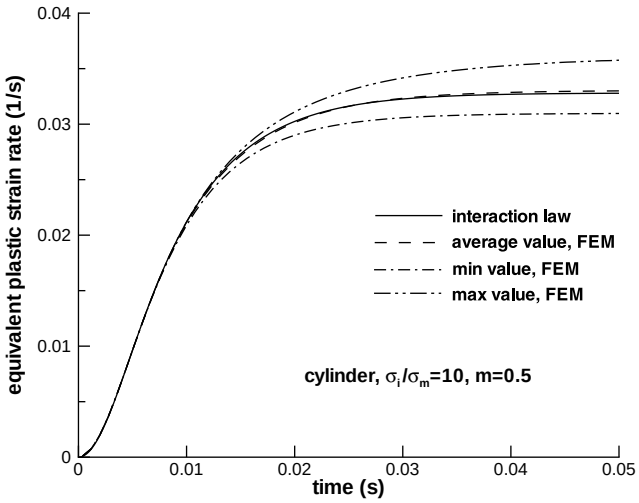

Fig. 14. Evolution of the equivalent plastic strain rate in a hard elongated inclusion (simulating a circular cylinder). The aspect ratio is large $\frac{c}{a} = 100, a = b$. Plane strain traction is applied at the remote boundary. Both phases have the same incompressible elastic behavior. The following material parameters are used: $m = 0.5$, $\mu = 66.66\,\text{MPa}$, $\sigma_m = 1\,\text{IS}$, $\sigma_i = 10\sigma_m$.

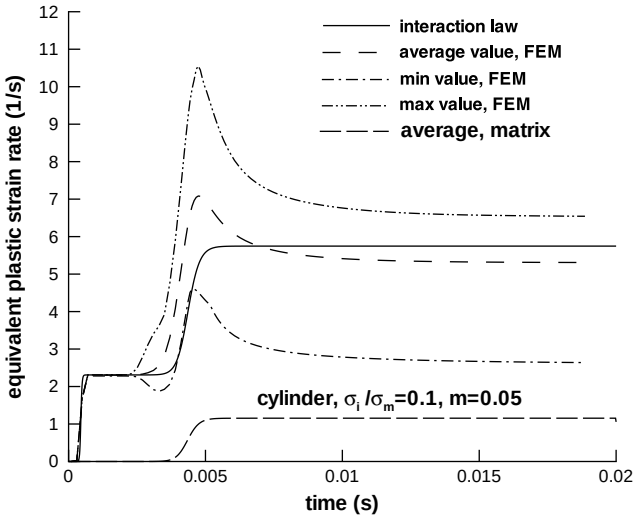

Fig. 15. Evolution of the equivalent plastic strain rate in a soft elongated inclusion (simulating a circular cylinder). The aspect ratio is large $\frac{c}{a} = 100, a = b$. Plane strain traction is applied at the remote boundary. Both phases have the same incompressible elastic behavior. The following material parameters are used: $m = 0.05$, $\mu = 66.66\,\mathrm{MPa}$, $\sigma_m = 1\,\mathrm{IS}$, $\sigma_i = 0.1\sigma_m$.

For $m = 1$, the two approaches coincide at any time. Thus, the difference between the viscoplastic interaction law and FE results of Gilormini and Germain (1987) mentioned by Molinari et al. (2004) for linear viscosity is really due to inaccuracy in the FE calculations (inaccuracy only observed for soft inclusions).

In the present paper, only two configurations are presented. The elastic behavior is assumed incompressible with $\mu_i = \mu_m = 66.66\,\mathrm{MPa}$. The strength of the matrix is $\sigma_m = 1\,\mathrm{IS}$. The inclusion is taken harder than the matrix $\sigma_i = 10\sigma_m$. The strain rate sensitivity is identical for both inclusion and matrix $m = 0.5$. A very good agreement between the two approaches is observed in Fig. 14. The last case concerns a soft inclusion $\sigma_i = 0.1\sigma_m$ (Fig. 15). A low strain rate sensitivity is adopted $m = 0.05$. As for spherical inclusions in axisymmetric loading, the prediction of the interaction law is in close agreement with FE results, except at intermediate times during the matrix transition from elastic to plastic regime.

4.2.2. Complex loading

Nonmonotonic loadings are now considered. Far field tensile loading is prescribed as in (13) during a time $t = 0.03\,\mathrm{s}$ and is replaced by shear loading (14) later in the deformation process. This shear loading breaks the symmetry with respect to axes $\underline{1}$ and $\underline{2}$ and the whole domain of the cross-section has to be meshed. The elastic behavior of the two phases is assumed incompressible with $\mu_i = \mu_m = 66.66\,\mathrm{MPa}$. The strength of the matrix is $\sigma_m = 1\,\mathrm{IS}$. The inclusion is harder than the matrix $\sigma_i = 1.5\sigma_m$. The strain rate sensitivity is identical for the two phases $m = 0.2$. In Figs. 16 and 17, the time evolution of respectively the total, plastic and elastic strain rate components are presented. A comparison between predictions based on the interaction law (4) and FE results is proposed for the total and the plastic strain rate. Fig. 18 shows a very good agreement for deviatoric stress components s_{11} and s_{12}. The evolution of the elastic strain rate d^{e}_{11} is also well predicted by the interaction law, even if FE results are not presented on Figs. 16 and 17 to gain in clarity. The beginning of the tensile loading is purely elastic with $d^{\mathrm{e}}_{11} = 1\,\mathrm{s}^{-1}$. This value is expected since both phases have the same elastic behavior. As time increases, a balance between elastic and viscoplastic deformation occurs. Later in the traction process, the deformation is purely viscoplastic with vanishing elastic deformation. At time $t = 0.03\,\mathrm{s}$, shear loading replaces tensile loading. A jump in the elastic strain rate component d^{e}_{11} from $0\,\mathrm{s}^{-1}$ to $-1\,\mathrm{s}^{-1}$ is observed. The elastic shear strain rate component d^{e}_{12} reaches

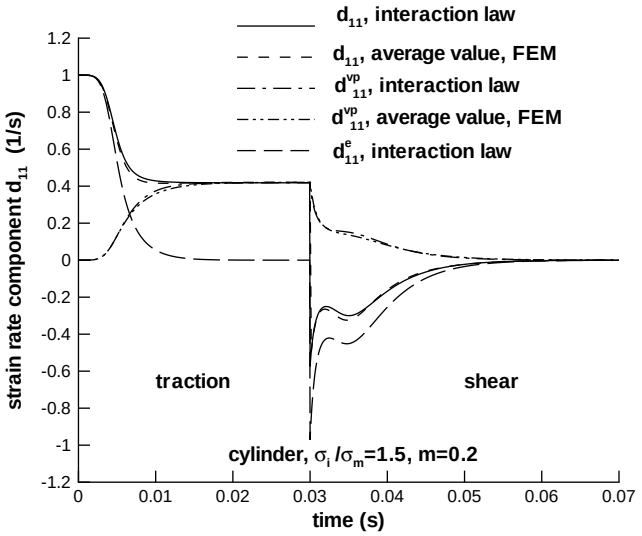

Fig. 16. Evolution of the total d_{11}, plastic d_{11}^{vp} and elastic d_{11}^{e} strain rate components in a hard elongated inclusion (simulating a circular cylinder). The aspect ratio is large $\frac{c}{a} = 100, a = b$. Complex loading is applied at the remote boundary: plane strain traction (13) during $t = 0.03\,\mathrm{s}$ followed by shear (14). Both phases have the same incompressible elastic behavior. The following material parameters are used: $m = 0.2$, $\mu = 66.66\,\mathrm{MPa}$, $\sigma_m = 1\,\mathrm{IS}$, $\sigma_i = 1.5\sigma_m$.

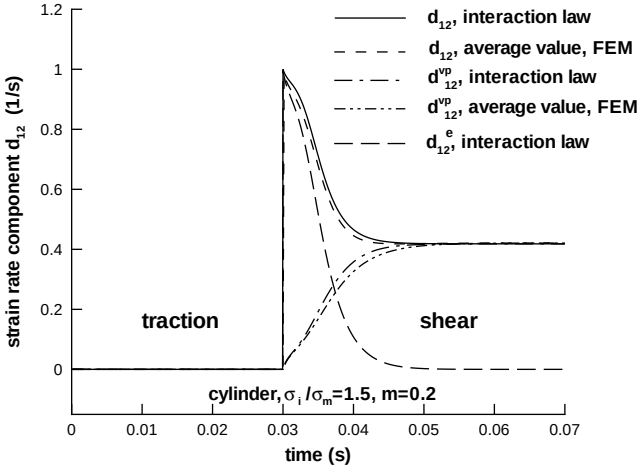

Fig. 17. Evolution of the total d_{12}, plastic d_{12}^{vp} and elastic d_{12}^{e} strain rate components in a hard elongated inclusion (simulating a circular cylinder). The aspect ratio is large $\frac{c}{a} = 100, a = b$. Complex loading is applied at the remote boundary : plane strain traction (13) during $t = 0.03\,\mathrm{s}$ followed by shear (14). Both phases have the same incompressible elastic behavior. The following material parameters are used: $m = 0.2$, $\mu = 66.66\,\mathrm{MPa}$, $\sigma_m = 1\,\mathrm{IS}$, $\sigma_i = 1.5\sigma_m$.

instantaneously the value $d_{12}^{\mathrm{e}} = 1s^{-1}$. Due to the elastic accomodation of the two phases, the viscoplastic strain rate component d_{11}^{vp} and the deviatoric stress component s_{11} are continuous and decrease slowly. They vanish at time $t = 0.06\,\mathrm{s}$. On the contrary, the viscoplastic shear strain rate d_{12}^{vp} and the deviatoric stress s_{12} increase monotonically and reach a plateau at time $t = 0.05\,\mathrm{s}$. Several tests have been performed with

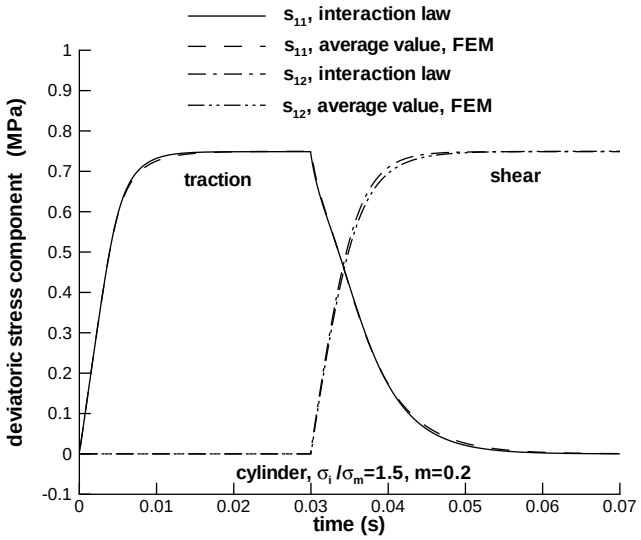

Fig. 18. Evolution of the deviatoric stress components s_{11} and s_{12} in a hard elongated inclusion (simulating a circular cylinder). The aspect ratio is large $\frac{c}{a} = 100, a = b$. Complex loading is applied at the remote boundary : plane strain traction (13) during $t = 0.03$ s followed by shear (14). Both phases have the same incompressible elastic behavior. The following material parameters are used: $m = 0.2$, $\mu = 66.66$ MPa, $\sigma_m = 1$ IS, $\sigma_i = 1.5\sigma_m$.

different hardness ratio and different strain rate sensitivities. When heterogeneity between the phases increases, the accuracy of the predictions based on the interaction law (4) decreases but remains good.

5. Conclusion

The aim of the present work was to validate an interaction law proposed by Molinari et al. (1997) for the Eshelby problem with elastic-viscoplastic materials. In the present approach, inclusion and matrix have elastic viscoplastic Maxwell behavior defined by relationships (1)–(3). The analytical solution of Hashin (1969) is retrieved when the behavior is linear and incompressible and when the inclusion is spherical. In the nonlinear domain, deformation heterogeneity within the inclusion has been quantified with FE simulations considering various inclusion shapes and different values of material parameters. Monotonic deformation paths such as axisymmetric tension, plane strain traction and nonmonotonic deformation pathes (tension-compression or tension-shear) have been considered. Elastic accomodation due to direction change in the deformation path is accurately predicted. It has been shown that, in general, the equivalent plastic strain rate in the inclusion predicted by the interaction law (4) is in good agreement with the average value derived from FE calculations (ABAQUS software). For soft inclusions, at initial and large times, the predictions are close to FE results. A difference is observed at intermediate times when the matrix undergoes a change from elastic to plastic regime. For hard inclusions, the difference reaches a maximum for large times i.e. during the viscoplastic domain when elastic strain rates are negligible. The results at large times match those obtained with the tangent interaction law for rigid viscoplasticity (elasticity neglected) proposed by Molinari et al. (1987). This simplified law offers an appropriate way to describe the response of an inclusion and has been widely used for simulations of texture evolutions in polycristalline materials.

In the present paper, time evolution of the average equivalent plastic strain rate inside the inclusion is shown for various configurations. Comparisons concerning other quantities such as the total strain rate,

the equivalent von Mises stress have been presented in Figs. 5(b) and 9 and similar conclusions can be drawn in general.

The present work demonstrates that elastic deformation can be included in a simple way in a realistic interaction law as expressed in (4). This law, which offers a good compromise between quality of results and computation time, is useful for the micromechanical modelling of elastic-viscoplastic heterogeneous materials. The information given by the interaction law is restricted to the first order moment of the elastic and viscoplastic strain rate per phase (volume averages). An open problem is still to find a way of estimating higher order moments so as to address the problem of strain heterogeneity per phase.

Appendix A. Equivalence of Eq. (7) with the analytical solution of Hashin (1969)

Matrix and inclusion are governed here by a linear Maxwell response. Introduction of Eqs. (5) and (6) into Eq. (7) in order to eliminate $\underline{d}_i$, $\underline{S}$ and $\dot{\underline{S}}$ leads to:

$$\dot{\underline{s}}_i\left(\frac{3}{2\mu_i}+\frac{1}{\mu_m}\right)+\underline{s}_i\left(\frac{3}{2\eta_i}+\frac{1}{\eta_m}\right)=5\underline{D} \tag{A.1}$$

where $\underline{D}$ (respectively $\underline{d}_i$) is the time derivative of the strain tensor $\underline{E}$ (respectively $\underline{\epsilon}_i$) since a small deformation theory is adopted. The Laplace transform of Eq. (A.1) provides the following relationship:

$$\hat{\underline{s}}_i(p)\left(\frac{3p}{2\mu_i}+\frac{p}{\mu_m}+\frac{3}{2\eta_i}+\frac{1}{\eta_m}\right)=5p\hat{\underline{E}}(p) \tag{A.2}$$

where p is the Laplace variable and $\hat{(.)}$ is the Laplace transform of the function (.).

The inclusion and matrix responses (5) are expressed in the Laplace space:

$$\hat{\underline{s}}_i(p)=2\hat{\mu}_i(p)\hat{\underline{\epsilon}}_i(p) \qquad \hat{\underline{s}}_m(p)=2\hat{\mu}_m(p)\hat{\underline{\epsilon}}_m(p) \tag{A.3}$$

where

$$\hat{\mu}_i(p)=\frac{\eta_i p}{1+\frac{\eta_i}{\mu_i}p} \quad \text{and} \quad \hat{\mu}_m(p)=\frac{\eta_m p}{1+\frac{\eta_m}{\mu_m}p} \tag{A.4}$$

The introduction of Eq. (A.3) into Eq. (A.2) gives:

$$\hat{\underline{\epsilon}}_i(p)=\frac{5\hat{\mu}_m(p)}{3\hat{\mu}_m(p)+2\hat{\mu}_i(p)}\hat{\underline{E}}(p) \tag{A.5}$$

The analytical solution in the Laplace space of the Eshelby problem is retrieved, Hashin (1969).

References

Eshelby, J.D., 1957. The determination of the elastic field of an ellipsoidal inclusion and related problems. Proc. Roy. Soc. Lond. A 241, 376–396.

Gilormini, P., Germain, Y., 1987. A finite element analysis of the inclusion problem for power law viscous materials. Int. J. Solids Struct. 23, 413–437.

Gilormini, P., Michel, J.C., 1999. Finite element solution of the problem of a spherical inhomogeneity in an infinite power law viscous matrix. Eur. J. Mech. A/Solids 17, 725–740.

Hashin, Z., 1969. The inelastic inclusion problem. Int. J. Engng. Sci. 7, 11–36.

Hill, R., 1965. Continuum micro-mechanics of elastoplastic polycrystals. J. Mech. Phys. Solids 13, 89–101.

Hutchinson, J.W., 1976. Bounds and self-consistent estimates for creep of polycrys-talline materials. Proc. Roy. Soc. Lond. A 348, 101–127.

Kouddane, R., Molinari, A., Canova, G.R., 1993. Self-consistent modelling of heterogeneous viscoelastic and elastoviscoplastic materials. In: Teodosiu, C., Raphanel, J., Sidoroff, F. (Eds.), Large Plastic Deformation. Balkema, Rotterdam, pp. 129–141.

Masson, R., Zaoui, A., 1999. Self-consistent estimates for the rate-dependent elastoplastic behavior of polycrystalline materials. J. Mech. Phys. Solids 47, 1543–1568.

Molinari, A., 2002. Averaging models for heterogeneous viscoplastic and elastic vis-coplastic materials. J. Engng. Mater. Technol. 124, 62–70.

Molinari, A., Ahzi, S., Kouddane, R., 1997. On the self-consistent modelling of elastic–plastic behavior of polycrystals. Mech. Mater. 26, 43–62.

Molinari, A., Canova, G.R., Ahzi, S., 1987. A self consistent approach of the large deformation polycrystal viscoplasticity. Acta Metall. 35, 2983–2994.

Molinari, A., Houdaigui, F.E., Toth, L.S., 2004. Validation of the tangent formulation for the solution of the non-linear eshelby inclusion problem. Int. J. Plasticity 20, 291–307.

Molinari, A., Toth, L.S., 1994. Tuning a self-consistent viscoplastic model by finite elements results-1 modeling. Acta Metall. Mater. 42, 2453–2458.

Paquin, A., Sabar, H., Berveiller, M., 1999. Integral formulation and self-consistent modelling of elasto-viscoplastic behavior of heterogeneous materials. Arch. Appl. Mech. 69, 14–35.

Rice, J.R., 1971. Inelastic constitutive relations for solids: an internal-variable theory and its application to metal plasticity. J. Mech. Phys. Solids 19, 433.

Rougier, Y., Stoltz, C., Zaoui, A., 1993. Représentation spectrale en viscoélasticité linéaire des matériaux hétérogènes. C. R. Acad. Sci. Paris, Serie II 316, 1517–1522.

Sabar, H., Berveiller, M., Favier, V., Berbenni, S., 2002. A new class of micro-macro models for elastic-viscoplastic heterogeneous materials. Int. J. Solids Struct. 39, 3257–3276.

Schapery, R., 1962. Approximate methods of transform inversion in viscoelastic stress analysis. In: Proceedings of 4th US National Congress on Applied Mechanics, Vol. 2, pp. 1075–1085.

Suquet, P., 1985. Elements of homogerieization for inelastic solid mechanics. In: Sanchez-Palencia, E., Zaoui, A. (Eds.), Homogeneization Techniques for Composite Media. Springer-Verlag, Berlin, pp. 193–278.

Turner, P.A., Tomé, C.N., Woo, C.H., 1994. Self-consistent modelling visco-elastic polycrystals: an approximate scheme. Phil. Mag. A 70, 689–711.

Weng, G.J., 1982. A unified, self-consistent theory for the plastic-creep deformation of metals. J. Appl. Mech. 49, 728–734.